

## Acoustic detection of laser induced melting of metals

M. Mesaros, O. E. Martínez, G. M. Bilmes, and J. O. Tocho

Citation: *Journal of Applied Physics* **81**, 1014 (1997); doi: 10.1063/1.364196

View online: <https://doi.org/10.1063/1.364196>

View Table of Contents: <http://aip.scitation.org/toc/jap/81/2>

Published by the *American Institute of Physics*

---

### Articles you may be interested in

[Quantitative measurements of laser-generated acoustic waveforms](#)

*Journal of Applied Physics* **53**, 4064 (1982); 10.1063/1.331270

[Measurement of laser-induced acoustic waves with a calibrated optical transducer](#)

*Journal of Applied Physics* **82**, 1525 (1997); 10.1063/1.365953

[Photoacoustic imaging in biomedicine](#)

*Review of Scientific Instruments* **77**, 041101 (2006); 10.1063/1.2195024

---



# Instruments for Advanced Science

Contact Hiden Analytical for further details:  
W [www.HidenAnalytical.com](http://www.HidenAnalytical.com)  
E [info@hiden.co.uk](mailto:info@hiden.co.uk)

**CLICK TO VIEW** our product catalogue



#### Gas Analysis

- dynamic measurement of reaction gas streams
- catalysis and thermal analysis
- molecular beam studies
- dissolved species probes
- fermentation, environmental and ecological studies



#### Surface Science

- UHV TPD
- SIMS
- end point detection in ion beam etch
- elemental imaging - surface mapping



#### Plasma Diagnostics

- plasma source characterization
- etch and deposition process reaction kinetic studies
- analysis of neutral and radical species



#### Vacuum Analysis

- partial pressure measurement and control of process gases
- reactive sputter process control
- vacuum diagnostics
- vacuum coating process monitoring

# Acoustic detection of laser induced melting of metals

M. Mesaros and O. E. Martínez<sup>a)</sup>

Departamento de Física, Facultad de Ciencias Exactas y Naturales, Universidad de Buenos Aires, Pabellón I, Ciudad Universitaria, 1428 Buenos Aires, Argentina

G. M. Bilmes

Centro de Investigaciones Ópticas-CIOp (CIC-CONICET) and Universidad Nacional de La Plata, Casilla de Correo 124, 1900 La Plata, Argentina

J. O. Tocho

Departamento de Física, Facultad de Ciencias Exactas, Universidad Nacional de La Plata and CIOp (CIC, CONICET), Casilla de Correo 124, 1900 La Plata, Argentina

(Received 3 June 1996; accepted for publication 10 October 1996)

Real time detection of pulsed laser surface melting was performed by analyzing the photoacoustic signals produced on the samples. Comparison between the amplitudes of the transversal and longitudinal waves allowed us to identify the fluence thresholds for surface melting. The method was tested with AISI 304 stainless steel samples and the results obtained were checked against direct metallographic analysis. © 1997 American Institute of Physics. [S0021-8979(97)03102-2]

Surface treatments by lasers and electrons beams are widely used in several processes of great technical and scientific importance. With these techniques, one key problem is to have real time control methods, which may allow one to decide when the energy densities used are sufficient to achieve some given process goal (surface melting, ablation, etc). Up to now, the great majority of characterization techniques (optical and electron microscopy, x-ray diffraction, etc.) require prior preparation; they cannot be carried out *in situ* and are time consuming. In the case of semiconductor samples, the change in the reflectivity upon melting is a well established *in situ* technique to determine the threshold.<sup>1-3</sup> To our knowledge this technique has not been applied to the case of metal surface melting because the change in the reflectivity of the metals during melting is not as large, and is masked by the larger change of the reflectivity of the solid with temperature.

Photothermal and photoacoustic techniques have, on the other hand, been successfully used to detect ablation thresholds or surface damage produced in metals irradiated by high power laser pulses.<sup>4,5</sup> Photoacoustic detection during ablation is based on the fact that the impulse transferred to the material by the ejection of the evaporated components produces very strong characteristic acoustic signals.<sup>6,7</sup> This type of characterization of surface changes is of great practical importance, mainly because photothermal techniques are inexpensive, nondestructive, and can be performed *in situ*.

Even though these techniques are very well known, little attention has been paid to photoacoustic detection of surface melting and to acoustic identification of surface melting thresholds.<sup>8</sup>

When there is not substantial damage of the surface (through material ablation or plasma formation), acoustic wave generation is mainly associated with thermoelastic effects.<sup>8,9</sup> In the case of laser irradiated metals, the absorption layer is extremely thin. This interaction produces strong thermal gradients normal to the surface of the solid. The

result is an acoustic source whose lateral dimensions (the region irradiated by the laser) are larger than the depth of penetration of heat inside the material.

It has been demonstrated<sup>10</sup> that the normal component of the thermal gradient contributes to the generation of both longitudinal and shear waves, and that strong lateral gradients mainly generate shear waves. Both mechanisms also contribute to the generation of surface waves or Rayleigh waves. As far as there is no plasma formation, the amplitude of the shear and longitudinal waves increase with increasing laser pulse energy.

In this work, by analyzing the photoacoustic signals produced by a Nd:YAG pulsed laser impinging on stainless steel samples, we identify the fluence thresholds for surface melting. To study the acoustic signals produced by laser action in metallic samples, the experimental setup sketched in Fig. 1 was used.

The beam of a Q-switched Nd:YAG laser (1064 nm, 100 mJ,  $\tau=15$  ns) was attenuated by the rotating polarizer P1 and the fixed polarizer P2, and was partially focused on the sample by the lens L (spot diameter 1 mm). A beam splitter

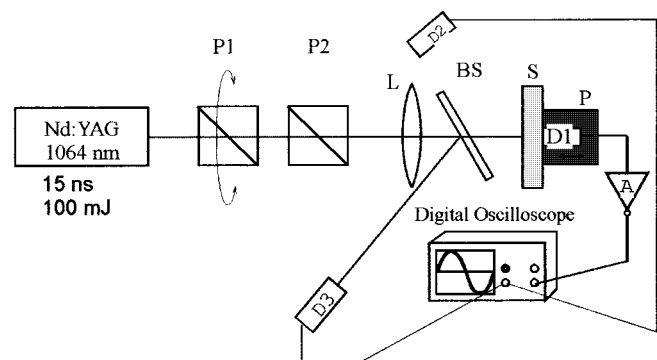


FIG. 1. Experimental setup. P1—polarizer, P2—polarizer, L—lens  $f=500$  mm, BS—beam splitter, S—sample, P—x-y positioning table, D1—piezoelectric transducer, D2—fast photodiode, D3—energy meter, A—amplifier  $\times 25$ .

<sup>a)</sup>Electronic mail: lecuba@df.uba.ar

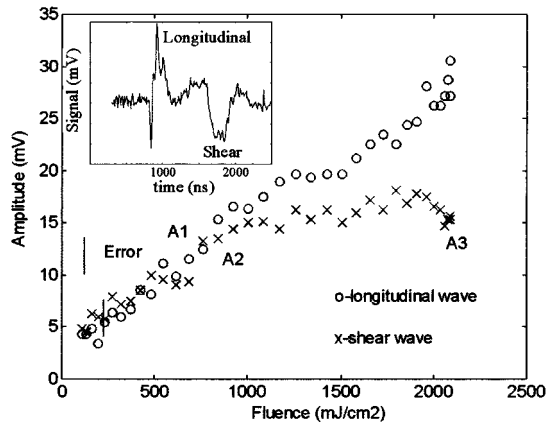


FIG. 2. Amplitudes of the longitudinal and shear acoustic waves. The inset shows a typical recorded signal.

BS and detector D3 were used to measure the energy of the laser pulse. The acoustic wave generated in the sample was detected by a nonringing, fast rise time polyvinylidene difluoride (PVF2) piezoelectric film transducer D1, of thickness  $9 \mu\text{m}$ . The film was mounted in a grounded enclosure to avoid electromagnetic interference as was described in Ref. 11. The acoustic signal detected was amplified  $25\times$  by the amplifier A and registered using the  $50 \Omega$  input of a digital oscilloscope of 175 MHz bandwidth. Photodetector D2 with a rise time of less than 5 ns, triggers the acquisition of data with a small reflection of the laser pulse.

The sample studied was an AISI type 304 stainless steel disk (weight composition 70 Fe, 18–20 Cr, 8–10 Ni, 0.08C) 5 mm thick and 50 mm in diameter. The thickness of the samples was chosen in such a way that the far field acoustic signal could be recorded.<sup>8</sup> In order to ensure this, the diffraction parameter

$$D = 2cz\tau/a^2 \gg 1, \quad (1)$$

where  $c$  is the sound velocity in the material,  $z$  is the thickness of the sample,  $\tau$  is the duration of the laser pulse, and  $a$  is the radius of the irradiated spot. The diffraction parameter in our experiment is  $D = 3.48$ . The advantage of measuring the far field acoustic displacement is that it is essentially proportional to the time derivative of the near field displacement. For instance, in absence of ablation, the expected far field longitudinal acoustic signal is bipolar.<sup>8</sup>

All samples were polished according to the usual techniques up to  $1 \mu\text{m}$  diamond powder.

In a series of measurements the time behavior of the acoustic signals was registered at fixed settings of the laser parameters and increasing energy densities on the sample.

A typical acoustic signal recorded is shown in the inset of Fig. 2. The longitudinal and the shear waves can be easily identified due to their different speeds of propagation. Peak to peak amplitude of the first longitudinal and shear wave was measured in the experiments as a function of the energy density impinging on the sample.

Figure 2 shows a plot of amplitude versus incident fluence in which three different regions can be identified. There is a first region (until approximately  $760 \text{ mJ/cm}^2$ ) in which

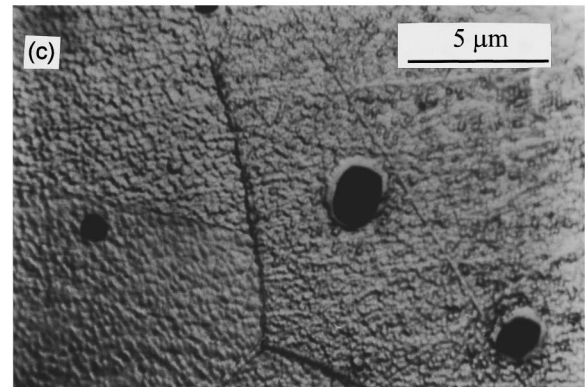
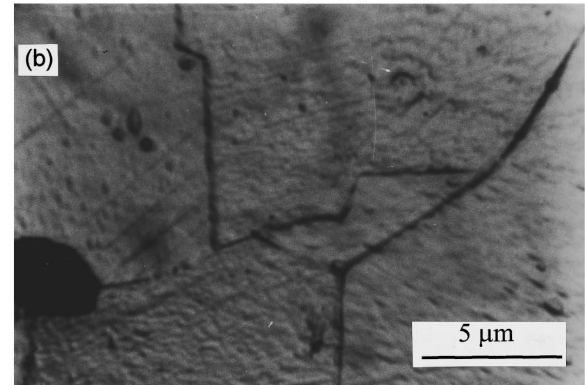
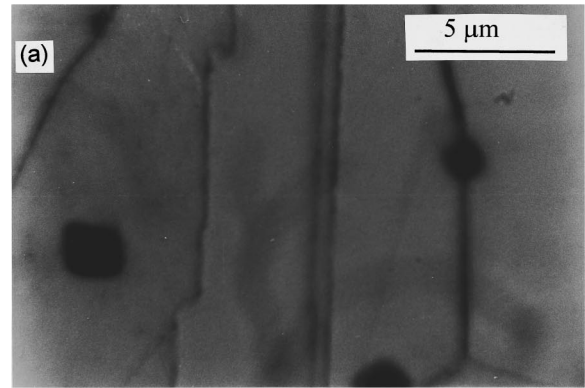


FIG. 3. Microphotographs of the irradiated areas in an AISI 304 stainless steel sample. (a) Fluence  $560 \text{ mJ/cm}^2$ , (b) fluence  $940 \text{ mJ/cm}^2$ , (c) fluence  $2000 \text{ mJ/cm}^2$

the two waves increase their strength in a similar way. In the second region the shear wave saturates while the longitudinal wave continues to grow (between  $760 \text{ mJ/cm}^2$  and  $1500 \text{ mJ/cm}^2$ ). This region will be identified as the melting zone because it is expected that the limited ability of fluids to transmit shear stresses would result in a saturation of the shear wave, while the longitudinal wave is nevertheless supposed to grow. In the third region, starting from  $1500 \text{ mJ/cm}^2$ , the material evaporates and after  $1800 \text{ mJ/cm}^2$  plasma formation takes place. These last two thresholds are easy to identify. When evaporation occurs, a characteristic noise is heard, and when plasma formation takes place a plume of evaporating material is observed. The error shown in Fig. 2 is mostly due to the jitter in the digitizing of the signal (100

Msamples/sec and will undoubtedly improve with a faster oscilloscope).

In order to check these thresholds and identify the fluences at which they can be produced, other samples were irradiated at 560 mJ/cm<sup>2</sup>, 940 J/cm<sup>2</sup>, and 2000 mJ/cm<sup>2</sup>, indicated in Fig. 2 as A1, A2 and A3, respectively. The irradiated samples were chemically etched to reveal their crystalline structure and to make a metallographic analysis. Micrographs of the irradiated areas are shown in Figs. 3(a), 3(b), and 3(c), all at the same magnification.

For fluence A1 (Fig. 3(a)) there is no visible superficial alteration. For fluence A2 (Fig. 3(b)) the surface seems corrugated. This corrugation is due to melting subsequent to the fast solidification. As further evidence, this corrugation extends up to grain boundary (and not up to the border of the irradiated area), indicating that it is not due to direct laser damage. For fluence A3 the damage can be seen by simple visual inspection even more clearly than at high magnification. Deep holes appeared, clearly distinct from the polishing pits seen in the samples prior to irradiation. The increase in the granularity due to evaporation is shown in Fig. 3 (c), and is similar to that found by Walters and Claver.<sup>12</sup>

In conclusion, we show a new real time technique for the identification of melting thresholds in laser irradiated metallic samples, based on the simultaneous detection of the lon-

gitudinal and transversal components of the photoacoustic signals generated. The results obtained by this technique, applied to 304 stainless steel samples irradiated with a Nd:YAG laser, show good correlation with direct metallographic analysis. The method developed is suitable for identification of melting thresholds in metallic samples of one phase, and with some care for the case of several phases, for which the analysis is more complex.<sup>13</sup>

<sup>1</sup>W. R. Sooy, M. Geller, and D. P. Bortfeld, *Appl. Phys. Lett.* **5**, 54 (1964).

<sup>2</sup>D. H. Auston, C. M. Surko, T. N. C. Venkatesaan, R. F. Slusher, and J. A. Golovchenko, *Appl. Phys. Lett.* **33**, 437 (1978).

<sup>3</sup>J. Solis, C. N. Afonso, and J. Piqueiras, *J. Appl. Phys.* **71**, (1992).

<sup>4</sup>A. P. Gosh and J. E. Hurst, *J. Appl. Phys.* **64**, (1988).

<sup>5</sup>P. E. Dyer and R. Srinivasan, *Appl. Phys. Lett.* **48**, 10 February (1986).

<sup>6</sup>C. B. Scruby, R. J. Dewhurst, D. A. Hutchins, and S. B. Palmer, *J. Appl. Phys.* **51**, 6210 (1980).

<sup>7</sup>R. J. Dewhurst, D. A. Hutchins, S. B. Palmer, and C. B. Scruby, *J. Appl. Phys.* **53** (1982).

<sup>8</sup>F. V. Bunkin, A. A. Kolomensky, and G. Mikhalevich, *Lasers in Acoustics* (Harwood Academic, Chur, Switzerland, 1990).

<sup>9</sup>D. Royer, M. H. Noroy, and M. Fink, *Proceedings of the 8th ITMP3*, 22–25 January 1994, Pointe-à-Pitre.

<sup>10</sup>A. M. Aindow, R. J. Dewhurst, D. A. Hutchins, and S. B. Palmer, *J. Acoust. Soc. Am.* **69** (1981).

<sup>11</sup>A. C. Tam, *Rev. Mod. Phys.* **58**, 381 (1986).

<sup>12</sup>C. T. Walters and A. H. Claver, *Appl. Phys. Lett.* **33**, 15 October (1978).

<sup>13</sup>M. Mesaros, O. E. Martínez, G. M. Bilmes, and J. O. Tocho, *Ann. Arg. Chem. Soc.* (to be published).